J. Chem. Eng. Data **2007,** *52,* 2117−2126

Adsorption of Alkanes and Aromatic Compounds on Various Faujasites in the Henry Domain. 1. Compensating Cation Effect on Zeolites Y

Xavier Canet,[†] Frederic Gilles,[‡] Bao-Lian Su,[‡] Guy de Weireld,[†] and Marc Frère*,[†]

Faculté Polytechnique de Mons, Thermodynamics Department, 31 bd Dolez 7000 Mons, Belgium, and Faculté Notre Dame de la Paix (FUNPD), Laboratory of Inorganic Materials Chemistry, 61 Rue de Bruxelles 5000 Namur, Belgium

Volatile organic compounds (VOCs) released in the atmosphere are responsible for important climate changes on earth, and some may have short- and long-term adverse health effects. The recovery of these VOCs can be a solution to reduce pollution. At low pressure, Henry constants are needed to develop recovery processes. Representative molecules were chosen to determine adsorption data. Nine alkanes (linear, cyclic, and branched molecules with carbon numbers between five and eight) and four aromatic and chlorinated compounds on a series of faujasite zeolites (HY, LiY, NaY, KY, RbY, and CsY) with the same Si/Al ratio were studied in the Henry domain at temperatures ranging from (448.15 to 673.15) K using the well-known pulse chromatography technique. The zeolites were characterized to determine the main structural properties such as cell parameters, chemical composition, porous volume, specific surface area, and water adsorption capacity. The Henry constant increases with rising cation size and probe molecule carbon number.

Introduction

Nowadays, reduction of atmospheric pollution is of prime importance. Volatile organic compounds (VOCs) released into the atmosphere by industrial activities and automobiles lead to some important environmental problems such as greenhouse effects and ozone layer destruction and can often modify the Chapman cycle (photochemical reaction) by reacting with nitrogen oxides in the air in the presence of sunlight and heat to form ozone which causes health effects in the troposphere by causing respiratory problems. VOCs are also responsible for direct health effects such as nausea, emesis, epistaxis, fatigue, allergic skin reactions, dyspnea, declines in serum cholinesterase levels, eye and respiratory tract irritation, headaches, dizziness, visual disorders, and memory impairment and may lead to leukaemia through prolonged exposure. Some VOCs are known to have carcinogenic, teratogenic, and mutagenic effects. A VOC is emitted as a gas from certain solids or liquids. A chemical is defined as a VOC if its vapor pressure is higher than 0.01 kPa at 293.15 K. VOCs are emitted by a wide array of products numbering in the thousands including paints, varnishes, and lacquers; paint strippers; cleaning, disinfecting, cosmetic, and degreasing products; pesticides; building materials and furnishings; office equipment such as copiers and printers; correction fluids and carbonless copy paper; graphics and craft materials including glues and adhesives; permanent markers; and photographic solutions. All of these products can release organic compounds during their use and, to some degree, when they are stored. Concentrations of many VOCs are consistently higher indoors (up to ten times higher) than outdoors. Organic chemicals are widely used as ingredients in household products and can be found in wood preservatives; aerosol sprays; cleansers and disinfectants; moth repellents and air fresheners; stored fuels and automotive products; hobby supplies; and dry-cleaned clothing.

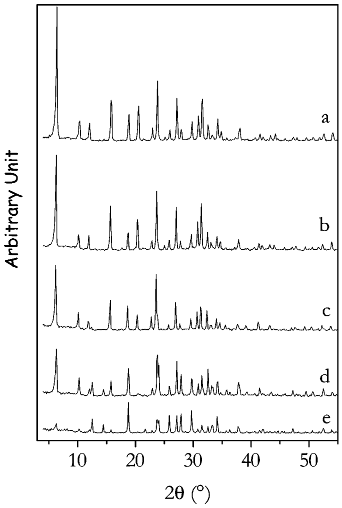

Figure 1. XRD diffraction patterns of Y zeolites exchanged with (a) Li^+; (b) Na^+; (c) K^+; (d) Rb^+; and (e) Cs^+ cations.

Table 1. Column Dimensions (Adsorbent Mass in g and Column Length in cm)

	alkane measurements		aromatic measurements	
	column length	adsorbent mass	column length	adsorbent mass
HY	3.76	0.258	2.98	0.209
LiY	3.97	0.266	2.48	0.161
NaY	4.66	0.337	2.29	0.155
KY	2.88	0.174	1.88	0.115
RbY	2.83	0.183	1.65	0.111
CsY	2.18	0.174	1.22	0.104

Ever increasingly stringent legislation has forced many companies to become tougher on measuring and controlling solvent emissions. For example, the Directive 2004/42/CE of the European Parliament and of the Council of 21 April 2004 deals with the limitation of emissions of volatile organic compounds due to the use of organic solvents in certain paints and varnishes and vehicle refinishing products. Thus, to reduce

---

* Corresponding author. E-mail: guy.deweireld@fpms.ac.be. Fax number: 0032/65/37 42 09.

[†] Faculté Polytechnique de Mons.

[‡] Faculté Notre Dame de la Paix (FUNPD).

10.1021/je700213m CCC: $37.00

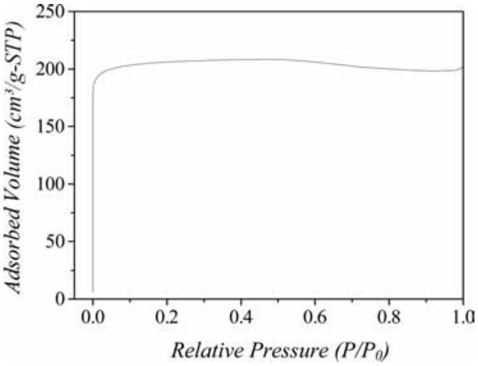

Figure 2. BET adsorption isotherm at 77 K for LiY.

Table 2. Adsorbent Characteristics (Chemical Composition, Specific Area, Si/Al Ratio, Cell Parameter "*a*", and Crystal Density)

	chemical composition	specific surface	Si/Al $m^2 \cdot g^{-1}$	*a* nm	crystal density $kg \cdot m^{-3}$
HY	$H_{56}Al_{56}Si_{136}O_{384}$	350	2.43		1241.0
LiY	$Li_{46}Na_{10}Al_{56}Si_{136}O_{384}$	717	2.43	2.48	1309.8
NaY	$Na_{56}Al_{56}Si_{136}O_{384}$	621	2.43	2.44	1405.9
KY	$K_{42}Na_{14}Al_{56}Si_{136}O_{384}$	631	2.43	2.46	1499.5
RbY	$Rb_{26}Na_{30}Al_{56}Si_{136}O_{384}$	551	2.43	2.41	1707.3
CsY	$Cs_{15}Na_{41}Al_{56}Si_{136}O_{384}$	446	2.43	2.42	1689.0

Table 3. Pore Volume ($cm^3 \cdot g^{-1}$), Dehydration Factors, and Adsorption Capacity of Water at Ambient Temperature ($g_{water}/g_{zeolite}$) for HY, LiY, NaY, KY, RbY, and CsY

zeolite	pore volume $cm^3 \cdot g^{-1}$	dehydration factor	adsorption capacity ($g_{water}/g_{zeolite}$)
HY	0.195	0.2486	0.331
LiY	0.385	0.2621	0.355
NaY	0.323	0.2461	0.326
KY	0.331	0.2162	0.276
RbY	0.290	0.1959	0.246
CsY	0.236	0.1736	0.207

Table 4. Dimensionless Henry Constant Data for Various VOCs at T = 448.15 K for HY, LiY, NaY, KY, RbY, and CsY

	HY	LiY	NaY	KY	RbY	CsY
2-methylbutane	207.5	413.7	686.0	1525.9	1927.9	2827.7
n-pentane	214.0	1298.7	1014.7	1554.8	2070.4	2858.9
cyclohexane	556.3	1255.8	1541.1	4276.9	6233.6	14175.1
2-methylpentane	690.0	1554.1	2194.9	5398.9	8409.2	12124.5
3-methylpentane	715.3	1622.0	2278.9	5362.6	8356.4	11644.5
2,3-dimethylbutane	703.3	1536.9	2207.9	5438.2	8345.6	13093.4
n-hexane	716.6	4749.4	4307.1	6359.7	8709.6	11461.7
n-heptane	1947.8	12920.3				
2,2,4-trimethylpentane		18309.7				

Table 5. Dimensionless Henry Constant Data for Various VOCs at T = 473.15 K for HY, LiY, NaY, KY, RbY, and CsY

	HY	LiY	NaY	KY	RbY	CsY
2-methylbutane	123.8	264.7	394.5	897.0	1084.0	1513.9
n-pentane	130.2	740.4	625.7	900.1	1162.8	1548.9
cyclohexane	307.9	701.7	897.5	2224.7	3349.0	6982.7
2-methylpentane	370.5	848.1	1160.6	2644.0	4295.7	5815.3
3-methylpentane	373.3	877.8	1196.1	2597.9	4173.9	5495.4
2,3-dimethylbutane	391.1	847.8	1192.8	2693.3	4125.9	6355.8
n-hexane	392.4	2232.8	2050.1	3444.5	4212.2	5377.4
n-heptane	990.9	6529.8	6256.2	11275.9	16341.4	24050.1
2,2,4-trimethylpentane	3671.5	8846.9	12047.2			

Table 6. Dimensionless Henry Constant Data for Various VOCs at T = 498.15 K for HY, LiY, NaY, KY, RbY, and CsY

	HY	LiY	NaY	KY	RbY	CsY
2-methylbutane	88.20	178.6	244.9	508.9	652.3	861.8
n-pentane	90.38	448.7	412.0	549.3	707.9	892.4
cyclohexane	194.4	435.9	542.7	1244.8	1855.8	3536.2
2-methylpentane	228.8	513.0	709.7	1464.4	2286.6	3053.7
3-methylpentane	229.2	519.6	722.0	1416.6	2241.6	2885.8
2,3-dimethylbutane	222.5	530.1	718.3	1373.6	2276.0	3338.7
n-hexane	232.1	1039.4	1088.7	1719.3	2299.6	2823.7
n-heptane	541.4	2791.8	3282.4	5077.7	8513.2	10168.4
2,2,4-trimethylpentane	1793.8	4572.0	6189.1	13278.7	18852.7	19914.9
chlorobenzene	2550.4	8529.5	17017.4			

Table 7. Dimensionless Henry Constant Data for Various VOCs at T = 523.15 K for HY, LiY, NaY, KY, RbY, and CsY

	HY	LiY	NaY	KY	RbY	CsY
2-methylbutane	61.44	127.7	166.9	330.1	443.1	533.1
n-pentane	65.65	277.3	248.1	347.3	471.1	540.3
cyclohexane	118.0	294.7	343.0	742.1	1213.2	1900.2
2-methylpentane	126.1	320.0	432.3	858.3	1347.4	1625.1
3-methylpentane	127.7	332.4	436.8	819.9	1353.4	1594.3
2,3-dimethylbutane	134.3	328.8	441.0	774.2	1342.4	1807.5
n-hexane	128.5	647.7	697.6	1010.4	1370.2	1605.7
n-heptane	294.5	1571.5	1685.5	2759.4	4417.6	5281.7
2,2,4-trimethylpentane	901.5	2462.6	3242.9	6524.5	8935.7	8362.9
chlorobenzene	1306.7	4703.9	8591.2	15282.4	31725.3	62761.9
toluene	2978.8	11185.7	17895.9	17324.5	26737.1	52117.6

Table 8. Dimensionless Henry Constant Data for Various VOCs at T = 548.15 K for HY, LiY, NaY, KY, RbY, and CsY

	HY	LiY	NaY	KY	RbY	CsY
2-methylbutane	45.54	92.0	130.0	222.3	313.1	353.0
n-pentane	46.25	180.4	171.8	235.5	322.2	349.7
cyclohexane	80.58	207.8	240.4	472.5	718.1	1095.1
2-methylpentane	84.58	218.8	275.2	518.8	831.3	912.2
3-methylpentane	83.88	233.2	278.4	499.6	833.5	973.3
2,3-dimethylbutane	88.28	224.0	284.4	512.7	838.1	1063.7
n-hexane	83.12	364.0	403.7	590.7	841.8	981.5
n-heptane	174.2	818.6	974.2	1595.0	2246.5	2749.7
2,2,4-trimethylpentane	493.2	1493.1	1851.5	3496.4	5052.2	4006.0
chlorobenzene	686.6	2372.9	4567.5	8519.0	16756.5	33320.9
toluene	1562.1	5971.0	9045.3	9442.9	14404.3	22897.1

these solvent emissions, the industry needs efficient filters and processes at both high and low concentration. Destructive techniques such as catalytic oxidation only change the pollution by throwing out another chemical compound, generally carbon dioxide which is responsible for global warming. Techniques such as cryogenics and absorption are used to recover VOCs but only at high concentration as they are not efficient at very low partial pressure.

Solutions for reduction or destruction of the VOCs have a very important energy cost and also throw out pollution. They are however currently very effective as long as the legislations on the emissions of VOCs are not very constraining. As the legislation will be increasingly severe, it will be necessary to use very effective recovery techniques at very low concentration. Adsorption will be used in industrial applications for purification of waste gases as the lower the pollutant concentration is, the more efficient adsorption is.

The determination of adsorption isotherms in the low partial pressure range for zeolite−VOC systems is then of prime importance for industry and science. Adsorption on microporous solids is a well-known technique for gas purification, often used after a cryogenic process to obtain high-purity gases. Consequently, the measurement of experimental data in the low-pressure range is the first step of any industrial process. Moreover, these data are quite important to understand adsorption mechanisms of the first molecules in the zeolite cages. Generally, isotherms of these kinds of systems are of type I.[1] These systems have a strong initial slope and a plateau covering almost the entire partial pressure domain. It is quite difficult to measure the first points of the isotherm because the initial slope

Table 9. Dimensionless Henry Constant Data for Various VOCs at $T = 573.15$ K for HY, LiY, NaY, KY, RbY, and CsY

	HY	LiY	NaY	KY	RbY	CsY
2-methylbutane	35.06	74.30	86.12	155.8	211.2	235.7
n-pentane	34.54	117.6	119.2	162.7	222.7	242.3
cyclohexane	58.24	148.0	167.1	328.0	510.5	692.8
2-methylpentane	60.54	159.0	206.4	366.3	539.0	538.1
3-methylpentane	63.40	159.3	211.8	348.1	545.0	559.7
2,3-dimethylbutane	64.53	160.2	213.4	375.5	550.2	622.8
n-hexane	59.35	249.5	263.2	396.0	556.7	539.1
n-heptane	114.6	543.1	579.9	929.0	1350.0	1558.7
2,2,4-trimethylpentane	299.3	887.1	1125.7	1962.8	2787.8	2035.3
chlorobenzene	400.4	1356.5	2535.6	4974.1	9807.0	16065.8
toluene	825.6	3524.8	4747.3	5228.0	8515.7	11922.8
m-xylene	2130.3	11577.9	19672.0	17030.7	22777.9	59013.8
p-xylene	1991.5	13862.0	18647.2	19689.1	30007.9	71209.5

Table 10. Dimensionless Henry Constant Data for Various VOCs at $T = 598.15$ K for HY, LiY, NaY, KY, RbY, and CsY

	HY	LiY	NaY	KY	RbY	CsY
2-methylbutane	28.54	59.72	68.35	117.7	160.7	164.1
n-pentane	28.46	90.10	93.16	122.9	166.9	167.5
cyclohexane	47.98	114.1	121.5	230.2	337.4	438.4
2-methylpentane	46.84	117.7	140.8	245.6	322.4	346.7
3-methylpentane	46.70	121.2	143.2	241.3	342.6	373.7
2,3-dimethylbutane	46.26	119.7	146.9	248.8	353.2	391.2
n-hexane	46.35	179.4	171.6	280.8	350.6	350.2
n-heptane	79.33	360.1	396.2	550.9	826.4	924.3
2,2,4-trimethylpentane	174.6	570.8	733.4	1229.2	1476.6	1137.2
chlorobenzene	260.6	827.0	1515.8	2981.5	5440.3	8575.9
toluene	465.7	2107.5	2710.8	3136.5	4906.8	6369.6
m-xylene	1160.4	6992.1	11597.1	9860.5	13016.1	26199.0
p-xylene	1060.8	7403.7	9766.9	10864.1	15263.7	29543.6

Table 11. Dimensionless Henry Constant Data for Various VOCs at $T = 623.15$ K for HY, LiY, NaY, KY, RbY, and CsY

	HY	LiY	NaY	KY	RbY	CsY
2-methylbutane	23.39	49.86	50.66	88.82	116.8	122.5
n-pentane	23.47	69.17	72.18	93.66	121.3	120.1
cyclohexane	35.59	87.29	96.40	160.7	236.4	291.4
2-methylpentane	33.56	83.34	109.1	173.7	237.7	227.0
3-methylpentane	34.74	85.38	111.0	170.3	233.9	242.4
2,3-dimethylbutane	35.91	83.60	111.8	179.3	235.8	260.4
n-hexane	33.95	127.8	121.6	180.8	240.9	227.3
n-heptane	57.89	233.8	268.6	387.4	526.0	559.5
2,2,4-trimethylpentane	113.2	393.5	489.7	784.8	895.4	627.5
chlorobenzene	154.5	556.6	966.1	1846.9	3357.5	4693.9
toluene	267.3	1286.3	1727.0	1839.2	2979.7	3619.3
m-xylene	612.9	3822.8	5986.7	5244.4	7928.8	12786.1
p-xylene	584.8	4240.8	5213.8	6070.4	8076.3	14272.6

Table 12. Dimensionless Henry Constant Data for Various VOCs at $T = 648.15$ K for HY, LiY, NaY, KY, RbY, and CsY

	HY	LiY	NaY	KY	RbY	CsY
chlorobenzene	108.5	355.4	606.9	1276.0	2203.1	2935.3
toluene	169.2	845.2	1126.0	1242.0	2003.4	2161.4
m-xylene	372.2	2522.6	3260.9	3206.7	5073.9	7267.3
p-xylene	352.1	2578.6	2881.8	3722.2	4977.6	8337.1

Table 13. Dimensionless Henry Constant Data for Various VOCs at $T = 673.15$ K for HY, LiY, NaY, KY, RbY, and CsY

	HY	LiY	NaY	KY	RbY	CsY
chlorobenzene	73.34	248.1	412.4	889.9	1440.8	1849.7
toluene	109.7	572.1	754.2	801.7	1308.9	1415.5
m-xylene	220.9	1561.8	1898.3	2028.9	3647.1	3854.3
p-xylene	203.1	1771.0	1715.6	2337.0	3171.1	4520.6

is in the very low partial pressure zone. The best zeolites for VOC adsorption in the Henry zone (the low partial pressure zone) have a quite important Henry constant; that is, the zeolite can adsorb a large number of molecules even at low concentration without being saturated.

Some previous work[2−14] provides interesting adsorption data on zeolites. These papers deal with specific adsorptives (nitrogen, argon, water, hydrocarbons, hydrofluorocarbons) and/or zeolites. Some of them aim at providing adsorption data for a specific application: xylenes separation,[2,3,10] air purification[7] and separation,[9] HFC separation techniques.[11] Others are focused on physical interpretation of adsorbate−adsorbent behavior.[3−6,8,12−14] It appears that a more general experimental study which would provide extensive results would be an interesting tool for further developments in the understanding of adsorption mechanisms and in predictive modeling.

This paper is devoted to the presentation of experimental adsorption data in the low partial pressure domain (Henry constant) for nine alkanes (linear, cyclic, and branched compounds) and four aromatic and chlorinated compounds used as probe molecules in the temperature ranges from (448.15 to 673.15) K and (448.15 to 623.15) K for alkanes, (523.15 to 673.15) K for aromatics, and (498.15 to 673.15) K for chlorobenzene carried out using the well-known pulse chromatographic method.[4−7,12,13,15−17] The adsorbents are monovalent cationic faujasite zeolites (HY, LiY, NaY, KY, RbY, and CsY) with the same Si/Al ratio to understand the effect of the compensating cation on the adsorption mechanisms of the initial molecules in the zeolite cages.

Experimental Section

Experimental Device and Procedure. The column filled with the adsorbent was located in the oven of an HP 5890 chromatograph equipped with a thermal conductivity detector (TCD). A purifier, filled with 3A zeolite, was placed in the system to remove water contained in the carrier gas (nitrogen with a purity higher than 99.999 %). Before any measurement, the temperature was raised to 673.15 K with a rate of 1 K per minute; this temperature was kept constant overnight under a flow of nitrogen to regenerate the adsorbent. A mass flow controller was used to regulate the flow of the carrier gas. After this regeneration step, the temperature was set to the experimental temperature. The hydrocarbon probe was injected with a syringe in the heated injector and passed through the column where it was adsorbed and desorbed, and then it goes to the TCD. The VOC concentration profile $c(t)$ at the column outlet was then recorded on a personal computer as a function of time t.

The mass of adsorbent in the column was determined by weighing the empty column and the column after degassing.

The details of the experimental procedure can be found in our previous work.[18]

Treatment of the Chromatographic Measurements. At the end of the experimental run, the following measurements were provided.

- Volumetric flow of inert carrier gas in the column.

- VOC concentration profile in the carrier gas vs time at the column outlet $c(t)$.

The first moment of this profile is related to the Henry constant by eq 1.[4−6,12,13,19]

$$\mu = \frac{V_{\text{column}}}{Q_{\text{T}}}[\epsilon + (1 - \epsilon)\rho_{\text{c}} \cdot RTK'] + \frac{V_{\text{d}}}{Q_{\text{T}}} \qquad (1)$$

with $\epsilon = \epsilon_{\text{i}} + \epsilon_{\text{p}}(1 - \epsilon_{\text{i}})$ and where μ is the retention time (s); V_{column} is the column volume (m^3); V_{d} is the dead volume between the injector and the detector (m^3); Q_{T} is the total volume flow (m^3·s^{-1}); T is the bed temperature (K); R is the ideal gas constant (J·K^{-1}·mol^{-1}); ϵ is the total porosity; ϵ_{i} is the interstitial

Table 14. Pre-exponential Factor of the van't Hoff Equation

	HY	LiY	NaY	KY	RbY	CsY
2-methylbutane	0.086533	0.201458	0.072204	0.055390	0.097852	0.037712
n-pentane	0.075837	0.031104	0.068694	0.063629	0.090904	0.035833
cyclohexane	0.029457	0.097338	0.070038	0.037208	0.057372	0.013186
2-methylpentane	0.013728	0.051568	0.046755	0.026578	0.024073	0.007990
3-methylpentane	0.014012	0.051043	0.045394	0.024704	0.027149	0.012543
2,3-dimethylbutane	0.015170	0.054151	0.051577	0.029097	0.029230	0.011020
n-hexane	0.011668	0.011101	0.013604	0.019701	0.027363	0.010646
n-heptane	0.005757	0.006939	0.011294	0.008863	0.009039	0.004398
2,2,4-trimethylpentane	0.001868	0.019888	0.018581	0.009659	0.005114	0.000719
chlorobenzene	0.003010	0.009341	0.010005	0.039261	0.029151	0.006746
toluene	0.000984	0.017671	0.011639	0.017419	0.035025	0.004681
m-xylene	0.000496	0.015516	0.002387	0.008755	0.087589	0.000730
p-xylene	0.000467	0.011591	0.001837	0.011162	0.007514	0.000747

Table 15. Adsorption Energy $-\Delta U$ (kJ·mol^{-1})

	HY	LiY	NaY	KY	RbY	CsY
2-methylbutane	28.73	28.22	33.91	37.98	36.68	41.69
n-pentane	29.40	39.60	35.80	37.56	37.25	41.97
cyclohexane	36.42	35.01	37.15	43.25	43.16	51.75
2-methylpentane	40.13	38.22	39.88	45.32	47.55	53.10
3-methylpentane	40.11	38.41	40.10	45.51	47.03	51.16
2,3-dimethylbutane	39.84	38.06	39.56	44.87	46.73	52.19
n-hexane	40.90	47.90	47.01	47.26	47.09	51.76
n-heptane	47.35	53.74	51.95	55.10	56.81	60.88
2,2,4-trimethylpentane	56.99	51.11	52.59	58.42	62.68	70.86
chlorobenzene	56.40	56.84	59.39	55.96	60.47	69.95
toluene	64.97	58.08	61.76	60.11	58.95	70.35
m-xylene	72.81	64.53	76.19	69.08	59.28	86.63
p-xylene	72.77	66.54	76.94	68.53	72.27	87.25

Table 16. Adsorption Enthalpy $-\Delta H$ (kJ·mol^{-1}) at 573 K

	HY	LiY	NaY	KY	RbY	CsY
2-methylbutane	33.49	32.98	38.67	42.74	41.44	46.46
n-pentane	34.17	44.37	40.56	42.32	42.01	46.74
cyclohexane	41.18	39.78	41.91	48.02	47.93	56.52
2-methylpentane	44.89	42.99	44.64	50.08	52.31	57.86
3-methylpentane	44.87	43.17	44.86	50.28	51.79	55.92
2,3-dimethylbutane	44.60	42.83	44.32	49.64	51.49	56.96
n-hexane	45.66	52.67	51.77	52.02	51.85	56.53
n-heptane	52.11	58.50	56.72	59.86	61.57	65.64
2,2,4-trimethylpentane	61.76	55.87	57.35	63.18	67.44	75.63
chlorobenzene	61.17	61.61	64.15	60.72	65.23	74.71
toluene	69.73	62.85	66.53	64.87	63.71	75.11
m-xylene	77.58	69.29	80.96	73.84	64.04	91.39
p-xylene	77.54	71.30	81.70	73.29	77.03	92.01

bed porosity; ϵ_p is the pellet macroporosity; ρ_c is the crystal density (kg·m^{-3}); and K' is the Henry constant (mol·kg^{-1}·Pa^{-1}).

Equation 1 may be written[18]

$$\mu = \frac{V_{\text{column}}}{Q_T}\left[1 - \frac{m_{\text{pellets}}}{V_{\text{column}} \cdot \rho_c} + \frac{m_{\text{pellets}}}{V_{\text{column}}} RTK'\right] + \frac{V_d}{Q_T} \qquad (2)$$

where m_{pellets} is the pellet mass in the column. μ was determined by the appropriate statistical treatment of $c(t)$. V_{column} and V_d were determined from metric measurements. ρ_c was calculated for an ideal crystal structure.

The Henry constant K' may be expressed in a dimensionless form, K

$$K = K' \rho_c RT \qquad (3)$$

The physical meaning of the Henry constants determined by this method implies an execution of the measurements in the Henry domain. The Henry domain is characterized by the fact that the retention time is not influenced by the injected volume. This is checked by performing several experimental runs with decreasing injected volumes of adsorbate for which we calculate the retention time. The linear correlation between the retention time and the inverse flow rate has to be verified: this is done by performing several runs with various gas flow rates. When the retention time does not depend on the injected volume and when the linearity between the retention time and the inverse flow rate was checked, the hypothesis of the column working in Henry's domain is valid. Typically, the injected volume is between (0.01 and 0.25) μL.

The van't Hoff plot of the dimensionless form of the Henry constant leads to the adsorption energy, given as

$$K = K_0 \exp\left(\frac{-\Delta U}{RT}\right) \qquad (4)$$

The maximum relative error in K is 8 % according to the error analysis.[18] K_0 is the pre-exponential dimensionless constant, and ΔU is the adsorption energy (J·mol^{-1}). The isosteric heat of adsorption at zero coverage, ΔH (J·mol^{-1}), is calculated by

$$\Delta H = \Delta U - RT \qquad (5)$$

Column Characteristics. For the measurements, the zeolite samples are pelletized in a press by applying a pressure of around 4.5 MPa. We use the (400 to 800) μm fraction to fill a 1/4 in. (6.35 mm) external diameter stainless steel column (length between (1 and 5) cm). The gas flow rates are between (1 and 2) Nl·h^{-1}. With such a column diameter and length, no pressure drop is measured in the apparatus. Table 1 gives the accurate column dimensions for each experimental run.

Adsorbents. All zeolites studied are faujasite type Y zeolites with different compensating cations (H^+, Li^+, Na^+, K^+, Rb^+, Cs^+) and crystallize in a cubic mode. The Si/Al ratio of these Y zeolites, provided by ^{29}Si MAS NMR, is 2.43.

The starting material is a NaY zeolite provided by Union Carbide. The Li^+-, K^+-, Rb^+-, and Cs^+-exchanged faujasites are obtained by ion exchange of the NaY material with a chloride solution of the corresponding alkali cation as described by Townsend.[19] The powder of the NaY zeolite is dispersed in a 6 M chloride solution. The suspension is then heated at 353.15 K over 4 h. The hot mixture is filtered and washed with distilled water to remove Cl^- ions. The full exchange process is repeated four times to obtain a good rate of exchange. The recovered material is finally dried in an oven at 393.15 K. A similar protocol is carried out to obtain NH_4Y using a 10 wt % NH_4NO_3 solution. After each exchange, a calcination is performed at 673 K for 6 h at a heating rate of 100 K per hour from room temperature in a flow of dry oxygen. The calcination is to decompose the NH_4^+ ions to give H^+, a small ion, to facilitate

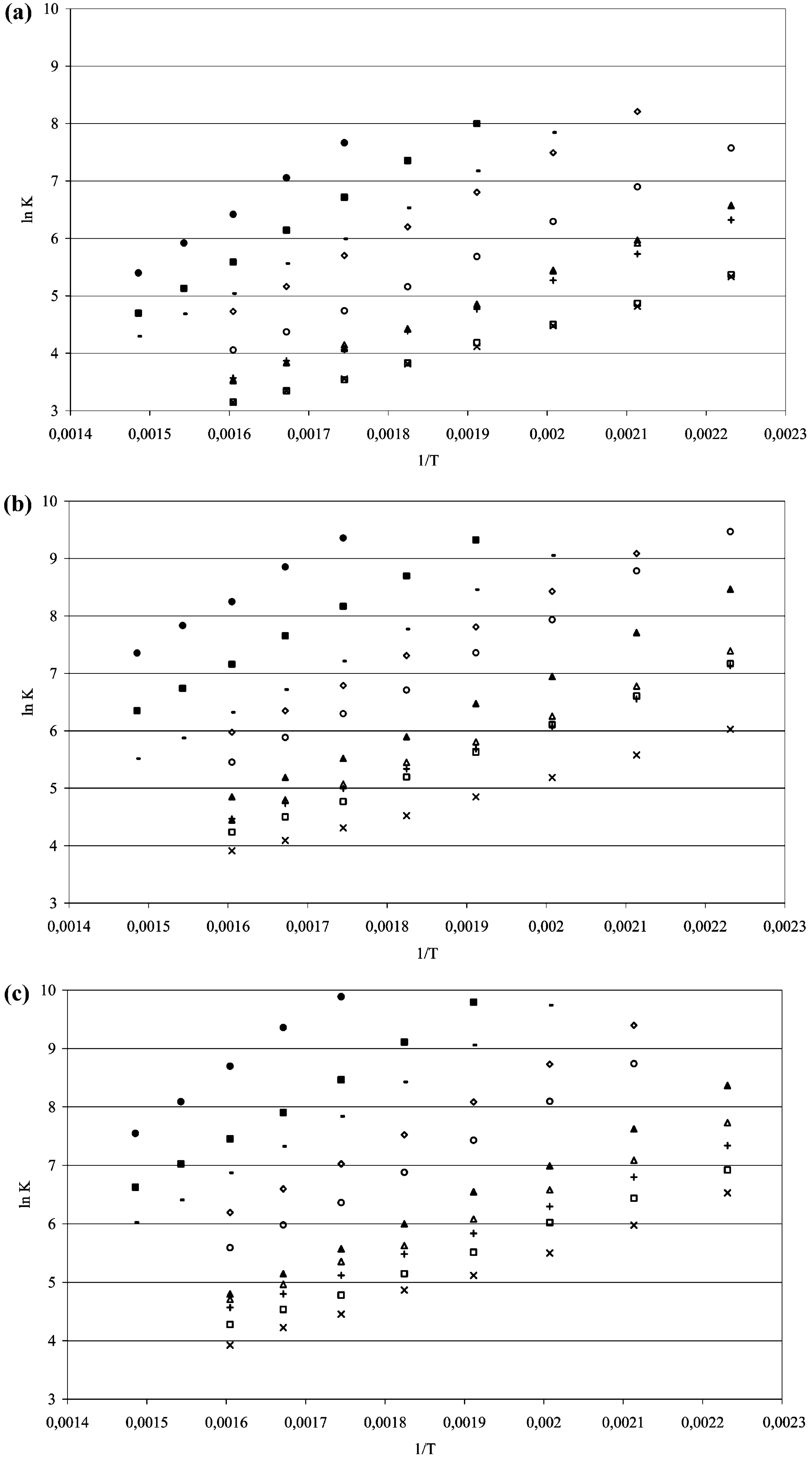
(a)
(b)
(c)
ln K
1/T
10
9
8
7
6
5
4
3
0,0014
0,0015
0,0016
0,0017
0,0018
0,0019
0,002
0,0021
0,0022
0,0023

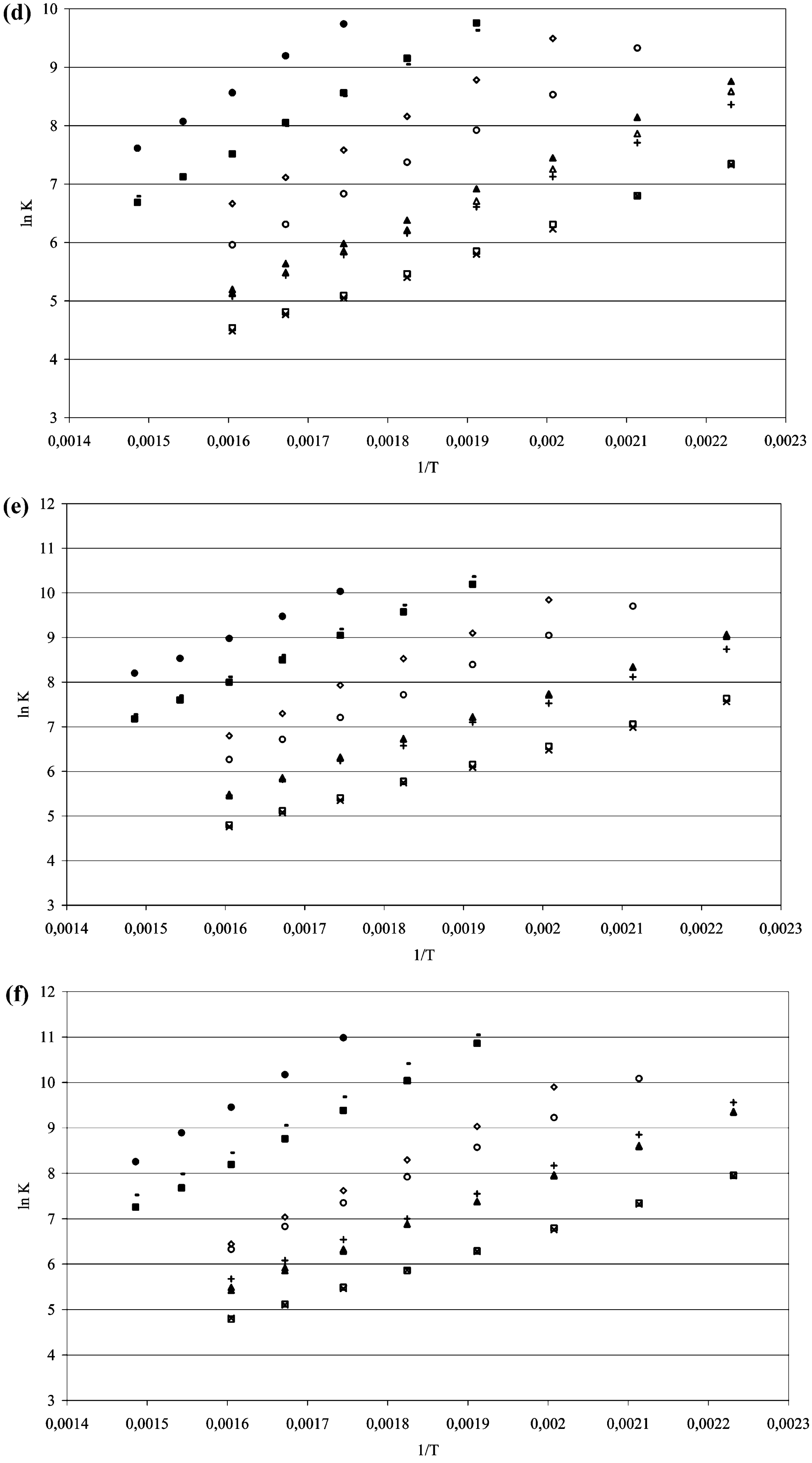

Figure 3. Plot of ln *K* vs 1/*T* for (a) HY, (b) LiY, (c) NaY, (d) KY, (e) RbY, and (f) CsY: x, 2-methylbutane; □, *N*-pentane; △, 3-methylpentane; ▲, *N*-hexane; ○, *N*-heptane; ◇, 2,2,4-trimethylpentane; +, cyclohexane; ■, toluene; ●, *meta*-xylene; and −, chlorobenzene.

the next exchange. The procedure is repeated seven times to obtain a 100 % rate of exchange.

The crystallinity of our materials was checked using an X-ray diffractometer (Philips PW 170) with a copper anticathode

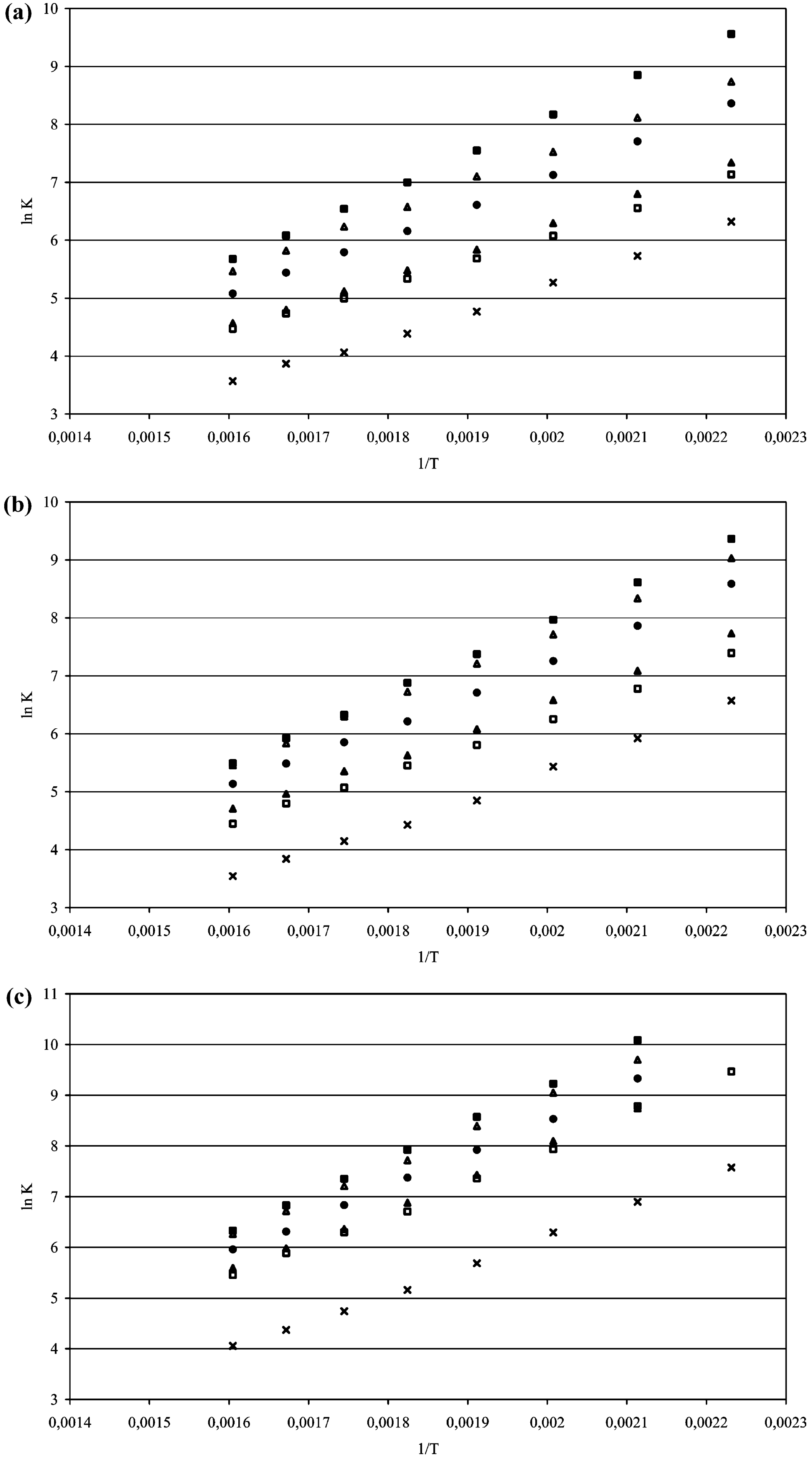
(a)
ln K
10
9
8
7
6
5
4
3
0,0014
0,0015
0,0016
0,0017
0,0018
0,0019
0,002
0,0021
0,0022
0,0023
1/T
(b)
ln K
10
9
8
7
6
5
4
3
0,0014
0,0015
0,0016
0,0017
0,0018
0,0019
0,002
0,0021
0,0022
0,0023
1/T
(c)
ln K
11
10
9
8
7
6
5
4
3
0,0014
0,0015
0,0016
0,0017
0,0018
0,0019
0,002
0,0021
0,0022
0,0023
1/T

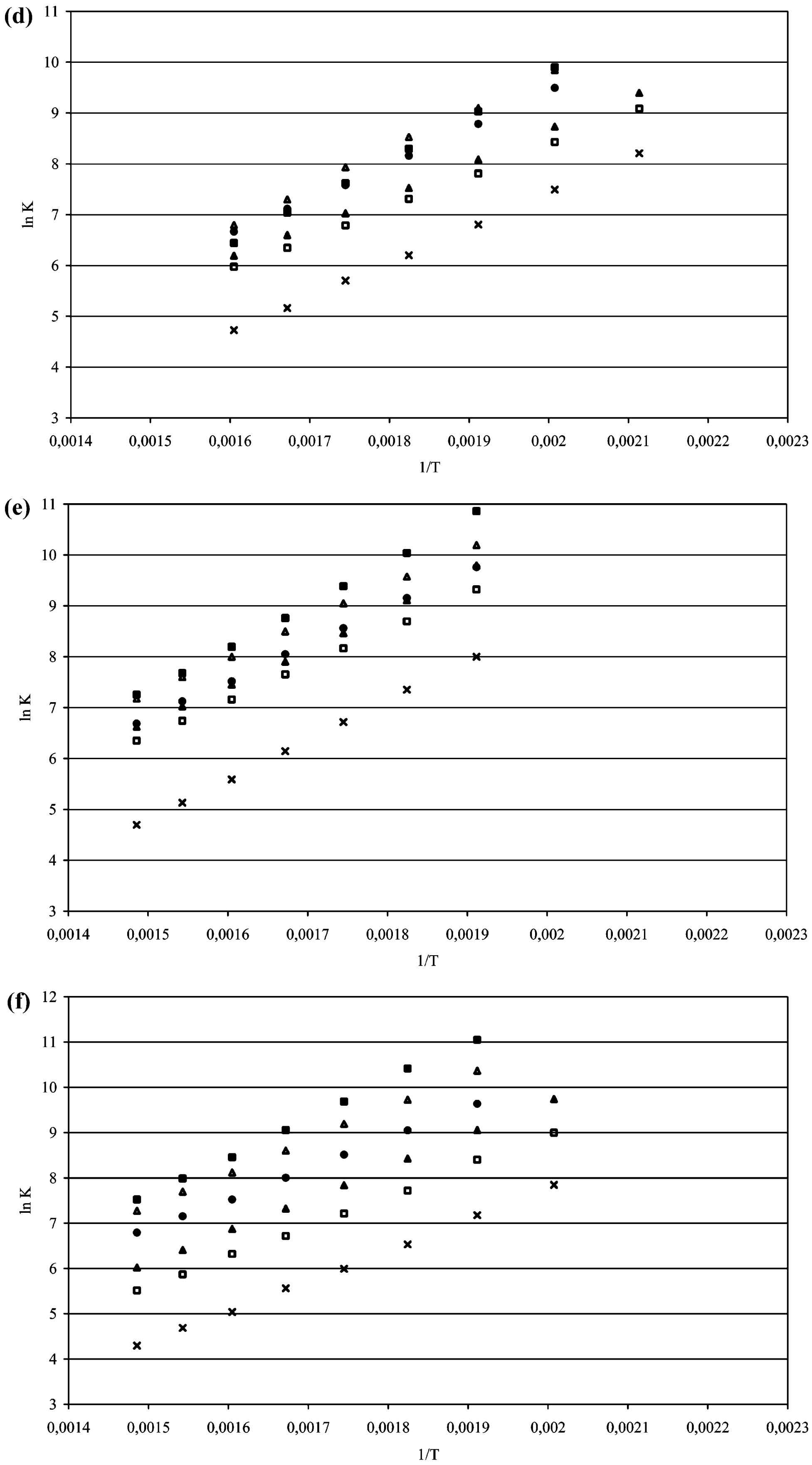

Figure 4. Plot of ln *K* vs 1/*T* for (a) cyclohexane, (b) 3-methylpentane, (c) *N*-heptane, (d) 2,2,4-trimethylpentane, (e) toluene, and (f) chlorobenzene: x, HY; □, LiY; ▲, NaY; ●, KY; △, RbY; ■, CsY.

producing X-rays with a wavelength equal to 1.54178 Å. Figure 1 presents the diffractograms of the starting material (Figure 1b) as well as those of the exchanged materials (Figures 1a and c to e). The XRD patterns of the exchanged faujasites are quite

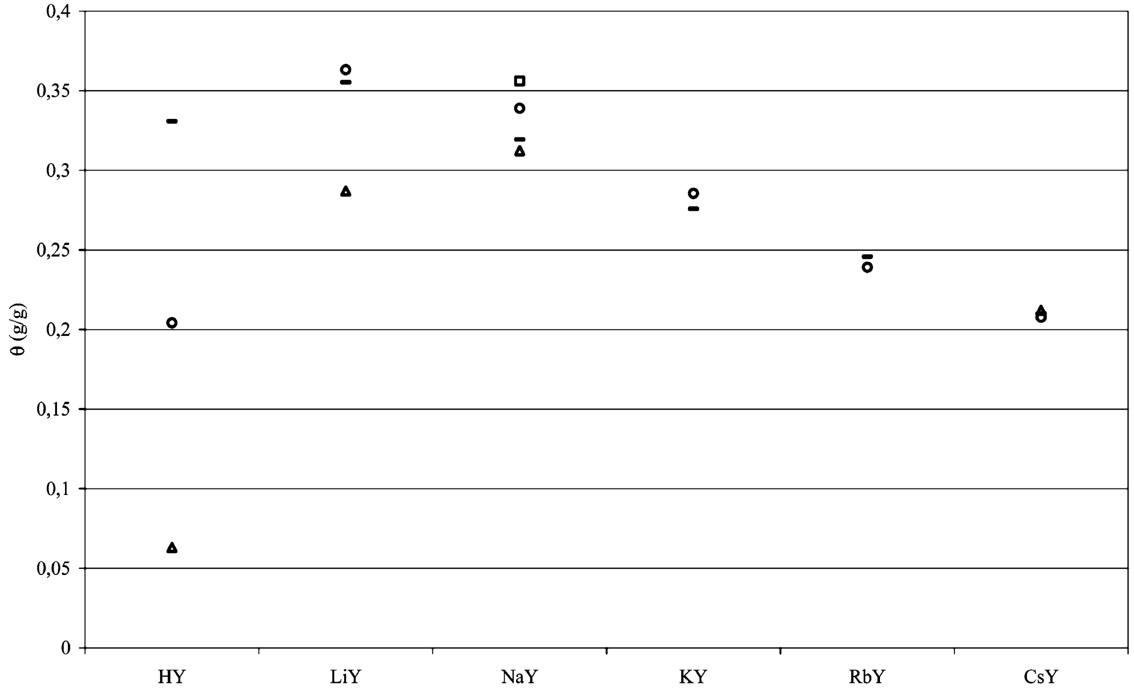

Figure 5. Adsorption capacity of water at ambient temperature for HY, LiY, NaY, KY, RbY, and CsY: −, this work; ◇, ref 13; △, ref 10; □, ref 9.

similar to that of the initial NaY sample. It is well-known that the introduction of a larger cation such as Cs^+ in the zeolitic framework can cause a modification on the zeolite framework and therefore on the XRD pattern. A decrease in intensity of the diffraction lines situated at low angle values is observed (Figure 1). The crystallite shapes of starting NaY particles are multifacetted spherulites, which are not altered by ion exchange.

Nitrogen adsorption−desorption isotherms were measured at 77 K on a Micromeritics ASAP 2010 instrument. All zeolites used have the same isotherm profile, and Figure 2 presents this isotherm for LiY. The samples were first degassed under a vacuum at 593.15 K for several hours. The Horvath−Kawazoe[21,22] method was used for the determination of the pore volume. The surface areas were determined using the BET equation in the low-pressure region (relative pressure between 0.05 and 0.25). The nitrogen adsorption−desorption isotherms, obtained on these materials, are typical of microporous materials with specific surface areas between (446 and 717) $m^2 \cdot g^{-1}$. A decrease in the specific surface area is observed when the size of the counterion is high. It is worth noting that the HK method used can slightly underestimate the pore size opening of the zeolites. Other more recent methods such as Saito−Foley and NLDFT could be applied for the precise calculation.[23] However, the utilization of the HK method will not change the trend of our present systematic study. Specific surface areas, chemical compositions determined by atomic absorption, and characteristics of all the studied samples are collected in Table 2. The cell parameter is determined by XRD.

The adsorbents are also characterized by their dehydration factor f defined by

$$f = 1 - \frac{\text{dehydrated mass}}{\text{total mass}} \qquad (6)$$

To measure the hydrated mass, the sample is left in contact with air at room temperature over a period of around 12 h. The dehydration is then performed by increasing the temperature up to 673.15 K (1 K per minute) in a chromatograph oven under a helium flow.

All these characteristics are gathered in Tables 2 and 3.

Adsorbates. The studied probes are alkanes (2-methylbutane, *n*-pentane, 2-methylpentane, 3-methylpentane, 2,3-dimethylbutane, *n*-hexane, *n*-heptane, 2,2,4-trimethylpentane, and cyclohexane) and aromatic compounds (toluene, *meta*-xylene, *para*-xylene, and chlorobenzene). All compounds are HPLC grade with purity higher than 99 % (toluene purity is higher than 99.8 %, and the purity of 2,2,4-trimethylpentane and cyclohexane is higher than 99.5 %).

The carrier gas used is nitrogen, as no different behavior is observed by using helium or nitrogen.

Adsorption Parameters. The experimental determinations of the Henry constants were achieved at temperatures ranging from (448.15 to 623.15) K for alkanes, from (523.15 to 673.15) K for toluene, from (498.15 to 673.15) K for chlorobenzene, and from (573.15 to 673.15) K for xylenes. Data points were taken at temperature intervals of 25 K.

The temperature dependence of the Henry constants for alkanes and aromatics on faujasites is presented in Tables 4 to 13 at temperatures from (448.15 to 673.15) K.

Figure 3 presents a plot of the logarithm of the Henry constant vs inverse temperature for all adsorbates on a given zeolite.

Figure 4 presents a plot of the logarithm of the Henry constant vs inverse temperature for a given adsorbate on all zeolites.

In comparing data for all faujasite zeolites and all compounds (alkanes and aromatics), the linear trend of ln K vs $1/T$ over the temperature range studied can be noticed. All plots are straight lines ($r^2 > 0.9995$).

We give the pre-exponential factor and the adsorption energy of the van't Hoff law in Tables 14 and 15. The adsorption enthalpy at 573.15 K is also given in Table 16.

As the studied zeolites are not completely exchanged, the interpretation of the experimental results is difficult, but the following statements can be made.

For all probes, the Henry constants increase with increasing cation size, and the general trend for the Henry constants is HY < LiY < NaY < KY < RbY < CsY. There is a large difference between HY and LiY Henry constants, and the NaY constants are close to those of LiY. As already explained,[11] "Li ions in site II buried between the oxygens of the six membered rings are inaccessible to the adsorbates whereas larger ions in site II are accessible to adsorbate molecules in the supercage". For HY, as the cation radius is smaller than Li^+, the adsorption is limited compared to LiY. As the Na^+ cation is bigger than Li^+, the cation is more accessible and adsorption is more important (the bigger the cation is, the higher the adsorption).

For alkanes, when the number of carbon atoms of the adsorbate increases, the Henry constants on a given zeolite increase too as already mentioned[4] for a NaY 2.7. Toluene is more adsorbed than iso-octane and less adsorbed than xylenes. When the cation size increases, a cross over on Henry's constants is observed between the two probes, toluene and chlorobenzene. For HY and LiY, toluene is more adsorbed at low partial pressure. For RbY and CsY, chlorobenzene has higher K constants. Any interesting selectivity can be seen for *meta*- and *para*-xylene separation on the zeolites used; that is, Henry's constants are almost the same for the two xylenes on a given zeolite.

On zeolites HY, KY, RbY, and CsY, the Henry constants and the heat of adsorption are almost the same for *n*- and iso-alkanes (monobranched alkanes or dibranched alkanes). Whereas for NaY and LiY zeolites, there is a small difference of K, the most significant K ratio or selectivity factor for NaY being 1.9 at 448 K. We have higher selectivity up to 3 for LiY at 448 K.

The selectivity factor is defined as

$$\alpha_{ij} = \frac{K_i}{K_j} \tag{7}$$

The adsorption capacity of water at ambient temperature can be compared to previous results[10,11,14] as shown in Figure 5. For all zeolites except HY and LiY, all results are close to previous work. For HY and LiY, the adsorption capacities are very different. HY is quite different because there is less than one cation per unit cell for these previous works.[11,14]

The comparison for HY is not possible as it is not the same zeolite. We can note that in the LiY case we are in agreement with Yang and Navrotsky[11] who have used a similar adsorbent with a Si/Al ratio of 2.5 but not with Savitz et al.[14] who have the same zeolite (Si/Al ratio of 2.43). The measurement of the water adsorption capacity at ambient temperature, simple apparently, led to variations that are very important according to the cases; it is not a good forecast for comparison of the results under more complex experimental conditions.

Conclusion

In this paper, we present adsorption data for nine alkanes (linear and branched) and four aromatics and chlorinated compounds on a homogeneous series of faujasite Y zeolites in the low partial pressure domain, that is, in the Henry region, under catalytic temperatures ranging from (448.15 to 673.15) K.

These measurements have been obtained using the well-known pulse chromatography technique. Some comments relating these results to the structural characteristics of the adsorbent are provided.

Literature Cited

(1) Sing, K. S. W.; Everett, D. H.; Haul, R. A. W.; Moscou, L.; Pierotti, R. A.; Rouquerol, J.; Siemieniewska, T. Reporting physisorption data for gas/solid systems with special reference for the determination of surface area and porosity. *IUPAC Pure Appl. Chem.* **1985**, *57*, 603−619.

(2) Bellat, J. P.; Simonot-Grange, M. H.; Jullian, S. Adsorption of gaseous p-xylene and m-xylene on NaY, KY and BaY zeolites: Part 1 Adsorption equilibria of pure xylenes. *Zeolites* **1995**, *15*, 124−130.

(3) Bellat, J. P.; Pilverdier, E.; Simonot-Grange, M. H.; Jullian, S. Microporous volume and external surface of Y zeolites accessible to p-xylene and m-xylene. *Microporous Mater.* **1997**, *9*, 213−220.

(4) Denayer, J. F.; Baron, G. V. Adsorption of normal and branched paraffins in Faujasite zeolites NaY, HY, Pt/NaY and USY. *Adsorption* **1997**, *3*, 251−265.

(5) Denayer, J. F.; Baron, G. V.; Martens, J. A.; Jacobs, P. A. Chromatographic study of adsorption of n-alkanes on zeolites at high temperature. *J. Phys. Chem. B* **1998**, *102* (17), 3077−3081.

(6) Denayer, J. F.; Souverijns, W.; Jacobs, P. A.; Martens, J. A.; Baron, G. V. High-temperature low-pressure adsorption of branched C5−C8 alkanes on zeolite Beta, ZSM-5, ZSM-22, zeolite Y and Mordenite. *J. Phys. Chem B.* **1998**, *102* (23), 4588−4597.

(7) Diaz, E.; Ordonnez, S.; Vega, A.; Coca, J. Adsorption characterization of different volatile organic compounds over alumina, zeolites and activated carbon using inverse gas chromatography. *J. Chromatogr. A* **2004**, 1049 139−146.

(8) Inel, O.; Topaloglu, D.; Askin, A.; Tumsek, F. Evaluation of the thermodynamic parameters for the adsorption of some hydrocarbons on 4A and 13X zeolites by inverse gas chromatography. *Chem. Eng. J.* **2002**, *88*, 255−262.

(9) Maurin, G.; Llewellyn, P. L.; Poyet, Th.; Kuchta, B. Adsorption of argon and nitrogen in X-Faujasites: qualitative relationships for understanding the interactions with monovalent and divalent cations. *Microporous Mesoporous Mater.* **2005**, *79*, 53−59.

(10) Moïse, J. C.; Bellat, J. P.; Methivier, A. Adsorption of water vapour on X and Y zeolites exchanged with barium. *Microporous Mesoporous Mater.* **2001**, *43*, 91−101.

(11) Savitz, S.; Siperstein, F. R.; Huber, R.; Tieri, S. M.; Gorte, R. J.; Myers, A. L.; Grey, C. P.; Corbin, D. R. Adsorption of hydrofluorocarbons HFC-134 and HFC-134a on X and Y zeolites: effect of ion-exchange on selectivity and heat of adsorption. *J. Phys. Chem. B* **1999**, *103*, 8283−8289.

(12) Ruthven, D. M.; Kaul, B. K. Adsorption of aromatic hydrocarbons in NaX zeolite. 1. Equilibrium. *Ind. Eng. Chem. Res.* **1993**, *32*, 2047−2052.

(13) Ruthven, D. M.; Kaul, B. K. Adsorption of n-Hexane and intermediate molecular weight aromatic hydrocarbons in LaY zeolite. *Ind. Eng. Chem. Res.* **1996**, *35*, 2060−2064.

(14) Yang, S.; Navrotsky, A. Energetics of formation and hydration of ion-exchanged zeolite Y. *Microporous Mesoporous Mater.* **2000**, *37*, 175−186.

(15) Askin, A.; Inel, O. Evaluation of the heat of adsorption of some n-alkanes on alumina and zeolite by inverse gas chromatography. *Sep. Sci. Technol.* **2001**, *36* (3), 381−397.

(16) Ruthven, D. M. *Principles of adsorption and adsorption processes*; John Wiley and Sons: Canada, 1984.

(17) Tümsek, F.; Inel, O. Evaluation of the thermodynamic parameters for adsorption of some n-alkanes on A type zeolite crystals by inverse gas chromatography. *Chem. Eng. J.* **2003**, *94*, 57−66.

(18) Nokerman, J.; Canet, X.; Mougin, P.; Limborg-Noetinger, S.; Frere, M. Comparative study of the dynamic gravimetric and pulse chromatographic methods for the determination of Henry constants of adsorption for VOC−zeolite systems. *Meas. Sci. Technol.* **2005**, *16*, 1802−1812.

(19) Canet, X.; Nokerman, J.; Frere, M. Determination of the Henry constant for zeolite−VOC systems using massic and chromatographic adsorption data. *Adsorption* **2005**, *11*, 213−216.

(20) Townsend, R. P. In *Introduction to Zeolite Science and Practice*; van Bekkum, H., Flanigen, E. M., Jansen, J. C., Eds.; Elsevier, Amsterdam, 1991; p 359.

(21) Hortvath, G.; Kawazoe, K. J. Method for calculation of effective pore size distribution on molecular sieve carbon. *J. Chem. Eng. Jpn.* **1983**, *16*, 470.

(22) Da Cruz, R. S.; E Silva, J. M. S.; Arnold, U.; Sercheli, M. S.; Schuchardt, U. J. Copper containing silicates as catalysts for liquid phase cyclohexane oxidation. *J. Braz. Chem. Soc.* **2002**, *13* (2), 170−176.

(23) Rouquerol, F.; Rouquerol, J.; Sing, K. *Adsorption by Powders and Porous Materials*; Academic Press: London, 1999.

Received for review April 24, 2007. Accepted July 21, 2007. This work was supported by the European Program of InterReg III (Programme France-Wallonie-Flandre, FW-2.1.5). The financial participation of Ministry of Environment and Natural Resources of the Walloon region to this program is acknowledged. This research was financially supported by Institut Français du Pétrole.

JE700213M